Atherosclerosis 281 (2019) 78–88

Contents lists available at ScienceDirect

Atherosclerosis

journal homepage: www.elsevier.com/locate/atherosclerosis

Decreased circulating catestatin levels are associated with coronary artery disease: The emerging anti-inflammatory role

Yanjia Chen[a,b,1], Xiaoqun Wang[a,1], Chendie Yang[a], Xiuxiu Su[a], Wenbo Yang[b], Yang Dai[b], Hui Han[a,b], Jie Jiang[a], Lin Lu[a,b], Haibo Wang[b], Qiujing Chen[b], Wei Jin[a,b,*]

[a] Department of Cardiology, Ruijin Hospital, Shanghai Jiao Tong University School of Medicine, 197 Ruijin 2nd Road, Shanghai, 200025, PR China
[b] Institute of Cardiovascular Diseases, Shanghai Jiao Tong University School of Medicine, 197 Ruijin 2nd Road, Shanghai, 200025, PR China

HIGHLIGHTS

- Serum catestatin (CST) level is inversely associated with CAD and disease severity.
- CST alleviates inflammation and improves EC dysfunction.
- Long-term CST administration attenuates the development of atherosclerosis.
- The anti-atherogenic effects by CST are mediated via an ACE2-dependent mechanism.

ARTICLE INFO

Keywords:
Catestatin
Hypotensive peptide
Atherosclerosis
Angiotensin-converting enzyme 2
Inflammation

ABSTRACT

Background and aims: The neuropeptide catestatin (CST) is an endogenous nicotinic cholinergic antagonist that acts as pleiotropic cardiac protective hormone. This study investigated the association between CST and coronary artery disease (CAD) and the underlying mechanisms.

Methods and results: The serum concentration of CST among 224 CAD patients and 204 healthy controls was compared, and its association with atherosclerosis severity in 921 CAD patients was further analyzed. Compared to healthy subjects, serum CST concentration was lower in patients with CAD [1.14 (1.05–1.24) ng/mL *vs.* 2.15 (1.92–2.39) ng/mL, $p < 0.001$] and was inversely correlated with disease severity ($r = -0.208$, $p < 0.001$). In cultured endothelial cells, CST suppressed TNF-α-elicited expression of inflammatory cytokines and adhesion molecules by activating angiotensin-converting enzyme-2 (ACE2). Administration of CST reduced leukocyte-endothelium interactions *in vitro* and *in vivo*, and attenuated the development of atherosclerotic in *ApoE*$^{-/-}$ mice fed a high-fat diet. These protective effects by CST were blocked by an ACE2 inhibitor.

Conclusions: Serum CST concentration is lower in CAD patients and is inversely associated with the severity of atherosclerosis. CST acts as a novel anti-atherogenic peptide that inhibits inflammatory response and EC-leukocyte interactions via an ACE2-dependent mechanism.

1. Introduction

Atherosclerosis is a chronic inflammatory disease that contributes to the majority of cardiovascular mortalities worldwide [1,2]. Overactivation of the sympathetic nervous system (SNS) leads to chronic mechanical injury to the arterial wall and development of atherosclerosis. Coronary endothelial dysfunction is part of a vicious cycle that increases the sympathetic tone, which may induce inflammatory responses and plaque rupture [3]. The atherosclerotic lesions can even be regarded as a consequence or complication of catecholamine actions [4]. (see Fig. 1)

Catestatin (CST), a 21-amino-acid-residue peptide, is derived from the neuroendocrine hormone chromogranin A (ChgA) [5,6]. This peptide is co-stored and co-released with catecholamine in adrenal chromaffin cells and adrenergic neurons. CST acts as an endogenous non-competitive antagonist of nicotine acetylcholine receptors, thereby inhibiting catecholamine secretion in mammals [7,8]. A substantial body of evidence shows that CST is a pleiotropic modulator against

* Corresponding author. Department of Cardiology, Ruijin Hospital, Shanghai Jiao Tong University School of Medicine, 197 Ruijin 2nd Road, Shanghai, 200025, PR China.
E-mail address: jinwei1125@126.com (W. Jin).
[1] These authors contributed equally to this work and should be considered co-first authors.

https://doi.org/10.1016/j.atherosclerosis.2018.12.025
Received 21 September 2018; Received in revised form 10 December 2018; Accepted 14 December 2018
Available online 24 December 2018
0021-9150/

cardiovascular diseases, such as essential hypertension [6,9], heart failure [10,11], and myocardial infarction [12,13]. These findings, together with the potential role of CST as an anti-endothelin-1 [14] and pro-nitric oxide agent *ex vivo* [15], suggest that the peptide may provide beneficial effects on the endothelium.

The renin–angiotensin system (RAS) is involved in multiple pathophysiological processes contributing to atherosclerosis [16] and has a mutual influence on the SNS [17]. The detrimental effects of RAS on the vasculature, including vasoconstriction, fibrosis, and inflammation, are activated by the engagement of angiotensin II (Ang II) to the Ang II type 1 receptor (AT_1R) [18]. The vasoprotective arm of the RAS includes angiotensin-converting enzyme 2 (ACE2), angiotensin-(1–7) [Ang-(1–7)], and Mas receptors [19]. A mutual regulation between RAS and ChgA-derived peptides has been identified. Vasoconstriction-inhibiting factor, a ChgA-degraded vasoregulatory peptide, modulates vasoconstrictive effects of angiotensin II by interaction with AT_2R [20]. On the other hand, RAS members possess enzymatic activity to hydrolyze ChgA [21]. In the present study, we hypothesized that CST may act as an endogenous protective peptide by counterbalancing the detrimental effects of RAS in preventing vascular injury and the development of atherosclerosis. The association of CST with the severity of coronary artery disease and its potential mechanisms were analyzed.

2. Materials and methods

2.1. Study population

To compare CST levels between patients with and without CAD, 224 patients with significant coronary artery disease (CAD) underwent baseline angiography were consecutively enrolled at the Department of Cardiology, Ruijin Hospital, Shanghai Jiao Tong University School of Medicine from May 2012 to December 2012. Significant CAD was defined as the visual identification of one major epicardial coronary artery with > 50% luminal diameter stenosis. The extent of CAD was graded based on angiographic results: by the number of diseased coronary arteries, with grades of 1–3 (namely, 1-, 2-, or 3-vessel disease). In particular, the left main coronary artery narrowing ≥50% was considered to be 2-vessel disease. Stable angina was diagnosed according to the criteria recommended by the American College of Cardiology and the American Heart Association [22]. Hypertension was defined as values ≥ 140 mmHg SBP and/or ≥90 mmHg DBP [23]. The diagnosis of diabetes was made according to the criteria of American Diabetes Association.

Another 204 subjects without evidence or history of vascular disease were served as controls. Such control subjects were from outpatient clinics around Rui Jin hospital and receiving an annual physical checkup. They had normal resting electrocardiogram and exercise stress test, as well as normal carotid artery ultrasound examination and echocardiography. To analyse the association of serum CST levels with the severity of atherosclerosis, we extended the enrolment period to February 2014. Thus, a total of 921 patients with CAD comprised the final CAD group.

For study purposes, patients with concomitant valvular heart disease, acute myocardial infarction, congenital heart disease, cardiomyopathy, acute and chronic viral or bacterial infections, pheochromocytoma, asthma, and cancer were excluded. All of the information, including age, lifestyle, medical history, and blood pressure, was collected using questionnaires.

The research was performed in accordance with the Declaration of Helsinki and was approved by the Ethics Committee of RuiJin Hospital, Shanghai Jiao Tong University School of Medicine. Informed consent for inclusion in the study was obtained from each of the participants.

2.2. Biochemical assessment

Blood samples were collected after an overnight fasting and were analyzed in the central laboratory of Ruijin Hospital. Blood samples were centrifuged at 2000 rpm for 20 min to collect the sera, which were then stored at −80 °C for further analysis. Serum CST levels were measured with a commercially available human CST enzyme-linked immunosorbent assay (ELISA) kit (catalog# 053-27, Phoenix Pharmaceuticals, Burlingame, California, USA), According to the manufacturer's instructions, the minimal detection limit for CST was 0.06 ng/ml and the cross-activity with the full-length chromogranin A molecule is 0%. No cross-activity was also confirmed by detecting CST levels with the ELISA kit in Chromogranin A protein samples. The serum glucose, liver function, blood urea nitrogen (BUN), serum creatinine (Scr), triglycerides (TG), total cholesterol (TC), high-density lipoprotein cholesterol (HDL-C), low-density lipoprotein cholesterol (LDL-C), and lipoprotein (a) (Lp(a)) were measured using a Hitachi 912 Analyzer (Roche Diagnostics, Germany).

2.3. Synthetic peptides, antibodies and reagents

Human CST (hCST) CgA352–372 (SSMKLSFRARGYGFRGPGPQL) was synthesized using a solid-phase method with 9-fluorenylmethoxycarbonyl protection chemistry [5,24]. The peptide was used at different doses from 0.1 to 10 μmol/L in the cell experiments and from 20 to 60 μmol/kg/day for intra-rectal injection in animal models [25,26]. Antibodies against angiotensin-converting enzyme 2 (ACE2, cat#ab15348), monocyte/macrophage-2 (MOMA-2), and monocyte chemo-attractant protein-1 (MCP-1, cat#ab151538) were purchased from Abcam (Cambridge, MA, USA) and analyzed with immunohistochemical assays and Western blots. Antibodies against matrix metalloproteinase-2 (MMP-2, cat#SC13595), MMP-9 (cat#SC6841), interleukin-6 (IL-6, cat#sc-1265-R), adhesion molecules including intercellular adhesion molecule-1 (ICAM-1, cat#4915s), vascular cell adhesion molecule-1 (VCAM-1, cat#12367s), and E-selectin (cat#sc-14011) and glyceraldehyde-3-phosphate dehydrogenase (GAPDH, cat#8884) were purchased from Cell Signalling Technology (Danvers, MA, USA) and Santa Cruz Biotechnology (Santa Cruz, CA, USA). Recombinant human tumour necrosis factor-α (TNF-α, cat#P01375) protein was purchased from R&D Systems. The ACE2-specific inhibitor DX600 (cat#002–55) was purchased from Phoenix Pharmaceuticals Inc. Radio-immunoprecipitation assay (RIPA) lysis buffer, phenylmethanesulfonyl fluoride (PMSF), and BCA protein assay kits were purchased from Beyotime (Shanghai, China).

2.4. Animal models

All of the animal experiments were performed according to the Shanghai Jiao Tong University School of Medicine's guidelines for the ethical care of animals. The protocol was approved by the Committee on the Ethics of Animal Experiments of the Shanghai Jiao Tong University School of Medicine (Permit Number: [2012]-86). Male ApoE-knockout ($ApoE^{-/-}$) mice (n = 50) at 8 weeks were purchased from Beijing Laboratory Animal Research Center and maintained in the Animal Experiment Center of RuiJin Hospital, Shanghai Jiao Tong University School of Medicine. All of the mice were housed in standard cages and kept on a 12-h light/12-h dark cycle with food and water freely available. The mice were fed with high-fat diet (HFD, 21% fat, 0.2% cholesterol, 23% protein, and 40.5% carbohydrates) throughout the experiment. To analyse the effect of CST on atherosclerosis, the mice were divided into 3 different treatments groups for 24 weeks: (i) the control group received intraperitoneal (i.p.) injection of PBS, (ii) the CST-treated group received i.p. injection of CST peptide (40 μmol/kg/day), and (iii) the CST + DX600 group simultaneously received i.p. injection of CST peptide (40 μmol/kg/day) and an ACE2-specific inhibitor, DX600 (0.1 μmol/L/kg/day; Phoenix Pharmaceuticals). The doses of CST and DX600 were chosen according to previously published data concerning the use of peptides for intra-peritoneal injections [26]. The mice were sacrificed after 24 weeks and the aortas were collected

for the subsequent pathological and biochemical analyses. Blood samples were drawn from the inferior vena cava in all groups. Serum levels of TC, TG, LDL-C, and HDL-C were measured enzymatically using commercially available kits (Shanghai Rongsheng Biotech Co., Ltd., China). Mouse body weight was also recorded.

2.5. Cell culture

Human aortic endothelial cells (HAECs) and human umbilical vein endothelial cells (HUVECs) (Cascade Biologics, Portland, OR, USA) were cultured in Medium 200 (Cascade Biologics) with low-serum growth supplements (Invitrogen, Carlsbad, CA, USA) and 5% fetal bovine serum at 37 °C in a humidified atmosphere of 5% CO_2. THP-1 monocytes were cultured in RPMI 1640 medium (Invitrogen, Carlsbad, CA, USA) containing 10% FBS, 100 μg/ml streptomycin, and 100 IU/ml penicillin at 37 °C in a humidified atmosphere of 95% air and 5% CO_2.

2.6. ACE2 siRNA transfection

An ACE2-specific siRNA (cat#sc-41400, Santa Cruz Biotechnology, Santa Cruz, CA) was transfected to knock-down ACE2 expression in the ECs. Briefly, HUVECs were seeded in a 6-well plate until 80% confluence. Cells were treated with lipofectamine/siRNA complexes, 1% FBS, and optiMEM (cat#31985-070, Gibco Thermo Fisher Scientific, US) for 20 min, followed by incubation in the fresh optiMEM for 6 h. A scrambled control siRNA (Santa Cruz Biotechnology, Santa Cruz, CA, USA) was employed as the negative control. Cells were harvested after 48 h of transfection. Protein expression levels of ACE2, IL-6, MMP-2, adhesion molecules (ICAM-1, VCAM-1, and E-selectin), and GAPDH were then analyzed by Western blots.

2.7. ACE2 activity assay

The ACE2 activity assay was performed using a microplate reader (BioTekSynergy™ 2; Biotek, Winooski, VT, USA). HUVECs were lysed in ACE2 buffer (75 mM Tris-HCL, 1 mol/L NaCl, and 0.5 μM $ZnCl_2$ at pH 7.5) and incubated for 10 min at 4 °C. The HUVECs were then centrifuged at 20,000 × *g* at 4 °C, and the supernatant was collected. The reaction mixture contained 50 μl supernatant, 5 mol/L NaCl, 10 μmol/L captopril, 50 μmol/L fluorogenic peptide substrate (Fluorogenic Peptide Substrate VI, R&D Systems), and ACE2 buffer, with a final volume of 100 μL. The fluorescence intensity was measured at an excitation wavelength of 330 nm and an emission wavelength of 390 nm. Specific ACE2 activity was determined by subtracting the readings in the presence of both 10 μmol/L captopril and 10 μmol/L DX600 from those with only captopril. The protein content of the samples was determined using a bicinchoninic acid (BCA) protein assay (Bio-Rad Laboratories, Hercules, CA, USA). The specific ACE2 activity was calculated by comparing the known amounts of recombinant human ACE2 (Calbiochem, Merck Millipore, Billerica, MA, USA) and them normalizing to the total protein.

2.8. Quantitative RT-PCR

The total RNA was extracted as described previously [27]. Briefly, 5 μg of total RNA was reverse-transcribed into cDNA using a reverse transcription system (Promega, WI, USA). PCR amplification was performed with the Power SYBR Green PCR Master Mix (Applied BioSystems, CA, USA) in a StepOne Real-Time PCR System (Applied BioSystems). The gene expression levels were normalized using *GAPDH*, and the data were analyzed using StepOne v2.1 (Applied BioSystems).

2.9. Monocyte-endothelial cell adhesion assay

HUVECs in 6-well plates were cultured for 24–48 h until 60% confluence and were divided into 6 treatment groups: 1) phosphate-buffered saline (PBS); 2) TNF-α (10 ng/ml); 3) TNF-α + CST (0.1 μmol/L); 4) TNF-α + CST (1 μmol/L); 5) TNF-α + CST (10 μmol/L); and 6) TNF-α + CST (1 μmol/L) + DX600 (1 μmol/L). We then added 2′7′-bis-(2-carboxyethyl)-5-(and-6)-carboxyfluorescein acetoxymethyl ester (BCECF-AM, Invitrogen, CA, USA)-labelled THP-1 monocytes (1×10^6 cells/ml) to all of the culture plates and incubated for 40 min at 37 °C to allow for cell interaction, followed by washing the non-adherent THP-1 cells with PBS. Cell attachment was observed by an inverted fluorescence microscope (IX50, Olympus). Monocyte-EC adhesion was calculated as the number of adherent monocytes per mm^2 area.

2.10. Intravital microscopy

Mice were anesthetized by intraperitoneal injection of pentobarbital sodium. CST (20, 40, and 60 μmol/kg), TNF-α (3 μg, as a positive control), DX600 (0.1 μmol/L/kg) or bovine serum albumin (BSA, 10 μg, as a negative control) was injected intraperitoneally 3 h before the operation. Leukocytes were fluorescently labelled by retro-orbital injection of 50 μl 0.05% rhodamine 6G (Sigma-Aldrich). Next, the mesenteric venules were exteriorized, and the rolling leukocytes were monitored using an inverted fluorescence microscope (IX71, Olympus) equipped with a stage warmer. Image-Pro V 6.2 (Media Cybernetics, Inc., Rockville, MD, USA) was used to automatically track real-time moving leukocytes. Leukocyte adherence was defined as a cell being stationary for at least 30 s. The leukocyte rolling flux was defined as the total number of leukocytes crossing the 100-μm venular segment in 1 min at a velocity that was significantly lower than the centerline velocity. Leukocyte rolling velocity was determined by measuring the time required for a leukocyte to roll along a 100-μm length of venule. Leukocyte adhesion is expressed as the number of cells/100 μm of venular length.

2.11. Histopathology and immunohistochemistry

Mice were anesthetized by intraperitoneal pentobarbital injections and perfused through the left ventricle with 0.9% NaCl followed by 4% paraformaldehyde under 100 mmHg. The aortic tissues were *en face* stained with Oil red O, and the percentage of lesion coverage was calculated by dividing the positively stained area by the total area. The aortic arches were prepared and analyzed using previously described methods [28]. Sections (5-μm thick) were routinely stained with Oil red O and Sirius red (Direct red 80, Sigma). Immunohistochemical analyses were performed to detect target protein expression levels of different treatment groups. In brief, endogenous peroxidase activity was inhibited by incubation with 3% H_2O_2. Sections were incubated overnight at 4 °C with primary antibodies and then incubated with secondary antibodies at 37 °C for 30 min. Visualization of positive reactions was developed using a peroxidase substrate solution that showed the reaction products as brown in color. The positive oil red O staining area relative to the total area of the entire aorta was measured to quantify the extent of the atherosclerotic lesions. Moreover, the cross-sectional lesion area relative to the total cross-sectional area of the aortic root was measured to estimate atherosclerosis severity.

The relative lipid, collagen, macrophage, and ACE2 contents were quantified as the ratio of the positive stained area to the total plaque area. Images were captured using an Olympus microscope and quantified using the image analysis software Image-Pro Plus 6.0.

2.12. Western blot analysis

Cell and tissue lysates were homogenized in RIPA lysis buffer containing 1% PMSF. After centrifuging the homogenates at 14,000 × *g* for 30 min at 4 °C, we collected the supernatant and assayed the protein concentration using a BCA protein assay kit. The supernatant was mixed with loading buffer and heated in a boiling water bath for 5 min.

Equal amount of prepared proteins was subjected to SDS-PAGE and blotted onto polyvinylidene fluoride membranes. The membranes were blocked with 5% non-fat milk in Tris-buffered saline with Tween-20 (Bio-Rad Laboratories, Inc., Hercules, CA, USA) and incubated overnight at 4 °C with antibodies against ICAM-1 (1:1000), VCAM-1 (1:1000), E-selectin (1:1000), IL-6 (1:1000), MMP-2 (1:1000), MMP-9 (1:1000), ACE-2 (1:1000), and GAPDH (1:2000). The membranes were then incubated with HRP-conjugated secondary antibodies (1:5000) for 1 h at room temperature. Immunoreactive bands were detected using an enhanced chemiluminescence (ECL) system (Millipore, MA, USA) and quantified using Image-Pro Plus 6.

2.13. Statistical analysis

Data are expressed as mean ± standard error of measurement (SEM) or median (inter-quartile range) for continuous variables, and frequencies (percentages) for categorical ones. For continuous variables, the existence of normal distribution was ascertained by the Kolmogorov–Smirnov test. Intergroup comparisons of categorical variables were performed using the $\chi 2$ test. Pearson's correlation testes were used to assess the relation between variables.

Different logistic regression analyses were implemented to assess the association of CST with the presence and severity of CAD. First, we analyzed the association between CST and CAD in the consecutively enrolled 224 CAD patients and the 204 age- and gender-matched healthy controls. Conventional risk factors were included in Model 1, including age, sex, smoking status, history of hypertension and diabetes, serum levels of triglyceride, total cholesterol, LDL-cholesterol, creatinine, troponin I, and ACEI/ARB use. In model 2, quartile of serum CST levels were further included. Second, logistic regression analysis was performed in the total 921 patients with CAD to interrogate the association of different CST quartiles with atherosclerosis severity. In model 1, univariate analysis was performed; in model 2, the association was adjusted by conventional risk factors including age, sex, smoking status, hypertension, diabetes mellitus and serum levels of triglyceride, total cholesterol, low density lipoprotein cholesterol, creatinine and troponin-I; in model 3, the association was further adjusted by ACEI/ARB use.

In vivo and *in vitro* data were quantified using Image-Pro Plus software and presented as means ± SEM. The sample size is documented in the respective Fig. legend. All of the analyses used 2-sided tests, and a $p < 0.05$ was considered to be statistically significant. Data analysis was performed using STATA 11.0 (Stata Corporation, College Station, TX, USA).

3. Results

3.1. Baseline clinical characteristics

The baseline characteristics of the subjects with CAD (224 subjects, the first part) and the healthy controls are presented in Supplementary Table 1. Compared with the healthy subjects, patients with CAD had increased prevalence of hypertension and diabetes, and elevated levels of lipoprotein (a), BUN, serum creatinine and troponin-I. Among all the CAD patients (all the 921 subjects), 421 had one-vessel disease, 268 had two-vessel disease, and 232 had three-vessel disease. The baseline clinical characteristics of the CAD population are summarized in Supplementary Table 2.

3.2. Serum CST levels are associated with CAD and atherosclerosis severity

Serum CST levels were lower in patients with than without CAD [1.14 (1.05–1.24) ng/mL *vs.* 2.15 (1.92–2.39) ng/mL, $p < 0.001$; Supplementary Fig. 1A]. A stepwise decrease in serum CST levels was found when classifying CAD patients into groups according to the number of diseased vessels: 1.95 (1.83–2.07) ng/mL in one-vessel disease, 1.57 (1.42–1.73) ng/mL in two-vessel disease, and 1.13 (1.00–1.27) ng/mL in three-vessel disease (p for trend < 0.001; Supplementary Fig. 1B). Moreover, log-transformed CST was inversely correlated to Gensini score ($r = -0.208$, $p < 0.001$, Supplementary Fig. 1C and D). After adjustment for age, sex, smoking habit, hypertension, diabetes, and serum concentrations of HDL-C, LDL-C, the correlation persisted significantly ($r = -0.196$, $p < 0.001$).

Multivariate logistic regression analyses showed that diabetes mellitus, biomeasurements including TG, serum creatine and cTNI were independently associated with the presence of CAD (model 1). After adjusting for risk factors and ACEI/ARB use in model 1, quartiles of CST concentrations remained inversely associated with CAD (p for trend < 0.001). Compared with the forth quartile, lower quartiles of CST corresponded to a dramatic increase in the odds ratio of CAD (1st quartile:10.4-fold, $p < 0.001$; 2nd quartile: 11.3-fold, $p < 0.001$; 3rd quartile: 1.6-fold, $p = 0.258$) (Table 1). In accordance, lower quartiles of CST were associated with higher presence of multivessle disease in CAD patients (p for trend < 0.01, 13.8-fold 1st *vs.* 4th quartile, $p < 0.001$) after adjustment for conventional risk factors and medication status (Supplementary Table 3).

Table 1
Multivariable regression analysis of independent risk factors for coronary artery disease.

Variable	OR (95%CI)	p value
Model 1		
Age	1.004 (0.977, 1.032)	0.799
Sex	0.570 (0.323, 1.006)	0.053
Smoking	1.093 (0.615, 1.941)	0.762
Hypertension	1.439 (0.847, 2.444)	0.179
Diabetes	4.700 (2.376, 9.300)	< 0.001
TG	1.400 (1.038, 1.888)	0.028
TC	0.794 (0.592, 1.066)	0.124
LDL-C	1.089 (0.900, 1.318)	0.381
Cr	1.025 (1.011, 1.039)	< 0.001
TNI	241.039 (1.31, 43000.219)	0.038
Medications on enrollment		
ACEI	0.433 (0.243, 0.769)	0.004
ARB	0.641 (0.326, 1.259)	0.197
Model 2		
Age	1.008 (0.977, 1.041)	0.611
Gender	0.478 (0.251, 0.909)	0.025
Smoking	1.122 (0.584, 2.156)	0.731
Hypertension	1.713 (0.931, 3.153)	0.083
Diabetes	3.905 (1.871, 8.148)	< 0.001
TG	1.410 (1.016, 1.955)	0.040
TC	0.762 (0.548, 1.061)	0.107
LDL-C	1.113 (0.900, 1.376)	0.325
Cr	1.024 (1.009, 1.039)	0.001
TNI	140.439 (1.022, 19289.641)	0.049
Medications on enrollment		
ACEI	0.475 (0.249, 0.909)	0.024
ARB	0.618 (0.288, 1.322)	0.215
Quartiles of CST		P_{trend} < 0.001
Quartile 1	10.374 (4.716,22.821)	< 0.001
Quartile 2	11.257 (4.853, 26.111)	< 0.001
Quartile 3	1.565 (0.721, 3.398)	0.258
Quartile 4	1	

OR (95% CI), Odds ratio (95% confidence interval) for coronary artery disease; TG, Triglycerides; TC, Total cholesterol; LDL-C, low-density lipoprotein-cholesterol; Cr, creatinine; TNI, troponin I; ACEI, Angiotensin-Converting Enzyme Inhibitors; ARB, Angiotensin-receptor blocker; CST, Catestatin.
Model 1, adjusted for conventional cardiovascular risk factors like age, gender, smoking, hypertension, diabetes mellitus, biomeasurements including TG, TC, LDL-C, Cr, TnI and medications on enrollment.
Model 2, adjusted for the factors included in Model 1 and quartiles of serum CST levels.

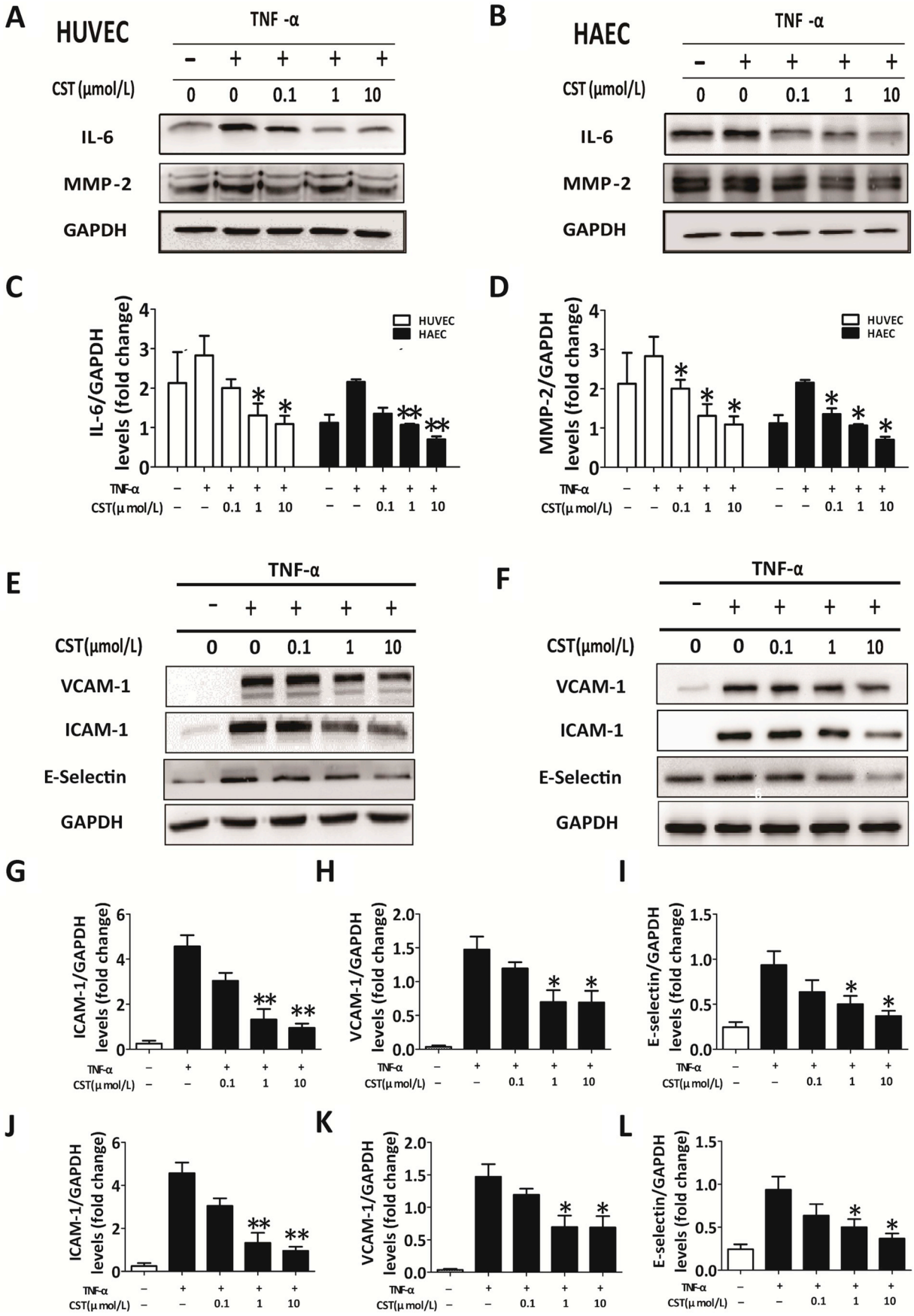

Fig. 1. Effect of catestatin on TNF-α-mediated inflammatory molecules and adhesion molecule expression in endothelial cells.

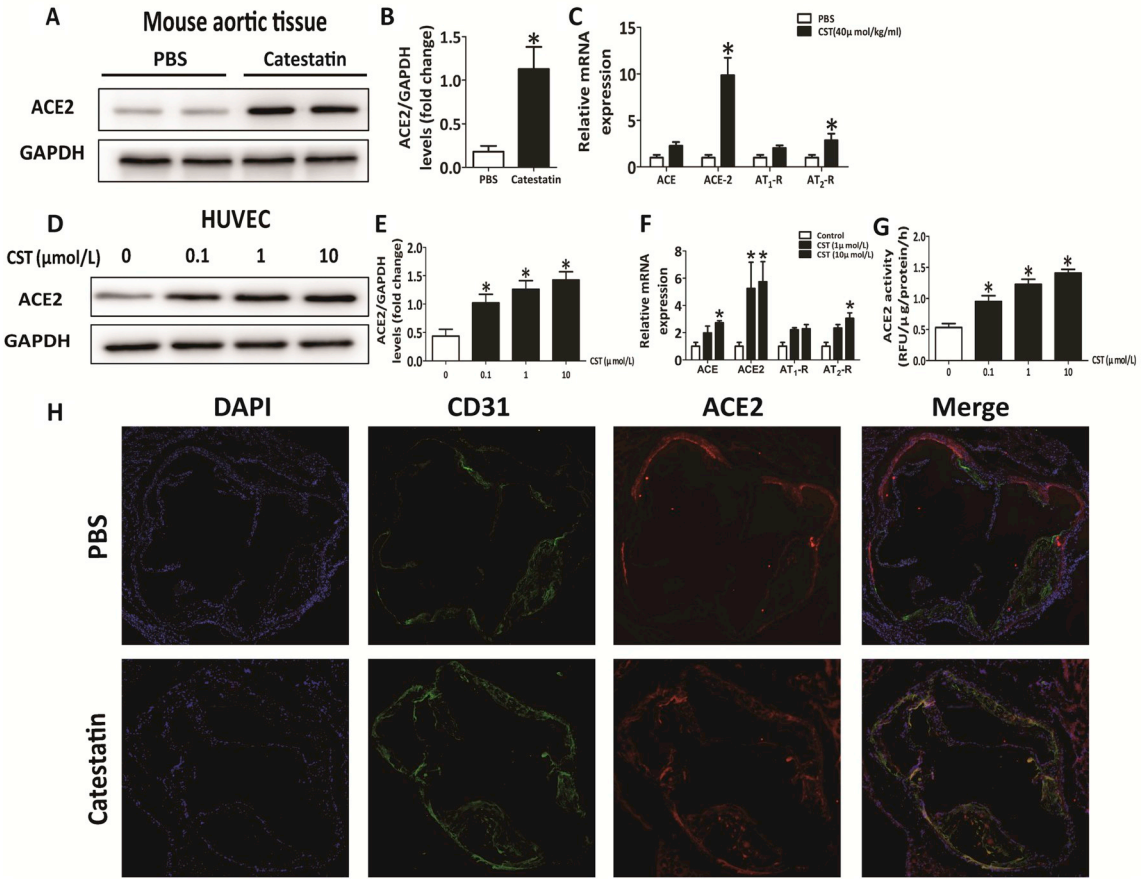

Fig. 2. CST increases ACE2 expression and activity in HUVECs and mouse aortic tissues.
(A) Representative blots showing ACE2 expression in mice treated with PBS or catestatin (CST, 40 μmol/kg/day). (B) Densitometric quantification of the Western blot results. (C) Relative mRNA expression levels of RAS members in mice treated with PBS and CST (40 μmol/kg/day). Data are expressed as the mean ± SEM ($n = 5$). *$p < 0.05$ *vs.* control mice treated with PBS. (D–G) HUVECs were treated with increasing doses of CST (0.1–10 μmol/L) for 24 h. Representative blots showing the expression levels of ACE2. (E) Densitometric quantification of the Western blots. (F) Relative mRNA expression of RAS members. (G) ACE2 activities measured in each treatment group. Data are expressed as mean ± SEM ($n = 6$). *$p < 0.05$ *vs.* control cells treated with PBS. (H) Representative images of ACE2 expression levels in mice treated with PBS or CST (40 μmol/kg/day). Endothelial cells were detected by CD31. Merge shows expression of CST in endothelial cells. Scale bar = 500 μm. ACE2, angiotensin-converting enzyme 2; PBS, phosphate-buffered saline; HUVECs, human umbilical vein endothelial cells; CST, catestatin; RAS, Renin-Aangiotensin System; TNF-α, tumour necrosis factor-α; DAPI, 4′,6-diamidino-2-phenylindole.

3.3. CST suppresses TNF-α-elicited EC dysfunction

Endothelial dysfunction is the initial event in the development of atherosclerosis. Thus, we conducted experiments to analyse the effects of CST on TNF-α-induced EC dysfunction. In cultured EC, a pronounced alleviation of TNF-α-induced expression of IL-6, MMP-2 and adhesion molecule (ICAM-1, VCAM-1, and E-selectin) was found in response to CST in a dose-dependent manner (Fig. 1), which was peaked at 10 mmol/L after treatment for 24 h (see Fig. 1).

3.4. CST increases ACE2 expression and activity

Infusion of CST was shown to result in prolonged vasodepression even after adrenergic blockade [29]. We therefore analyzed whether CST interferes with RAS associated with vascular inflammation [30,31]. In C57BL/6 mice, CST administration led to a significant increase in expression levels of ACE2 and AT_2-R (protein: Fig. 2A–2B; mRNA: Fig. 2C), but had no effects on ACE and AT_1-R. Consistently, CST promoted both the expression and activity of ACE2 in a dose-dependent manner in HUVECs (Fig. 2D–2G). Immunofluorescence analysis indicated that ACE2 expression in the atherosclerotic plaques was higher in the CST-treated mice than the control animals (Fig. 2H).

3.5. CST alleviates leukocyte-endothelium interactions in an ACE2-dependent manner

Rolling and adhesion of leukocytes along the endothelium initiate infiltration of inflammatory cells to the arterial wall and thereby the development of atherosclerosis. By using intravital microscopy, we found CST evidently reduced adhesion events and increased the rolling velocity of fluorescently labelled leukocytes in the mesenteric venules. Importantly, these beneficial effects were markedly abolished by co-administration of an ACE2 inhibitor, DX600 (Fig.s 3A–3D). Accordingly, CST inhibited the TNF-α-induced THP-1 adhesion to HUVECs *in vitro* in a dose-dependent manner, which was also blunted by DX600 (Figs. 3E and 4F).

3.6. ACE2 inhibition diminishes the anti-inflammatory effects of CST

HUVECs were then pretreated with DX600 to test if the anti-inflammatory effect of CST was mediated by ACE2. We found the inhibitory effect of CST on TNF-α-elicited inflammatory cytokine expression was markedly mitigated (Fig. 3G), to a similar extent by knockdown of ACE2 with a specific siRNA (Fig. 3H, Supplementary Fig. 2).

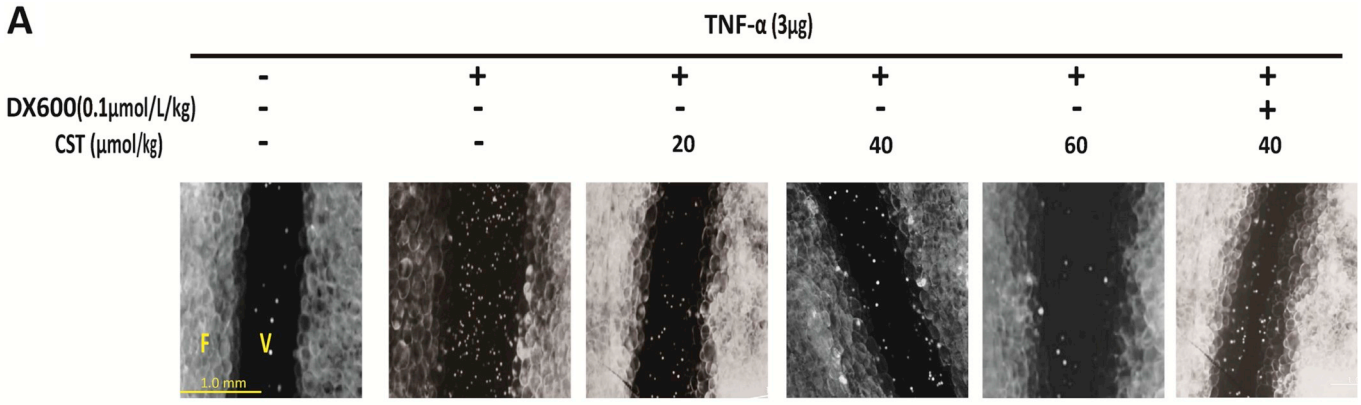

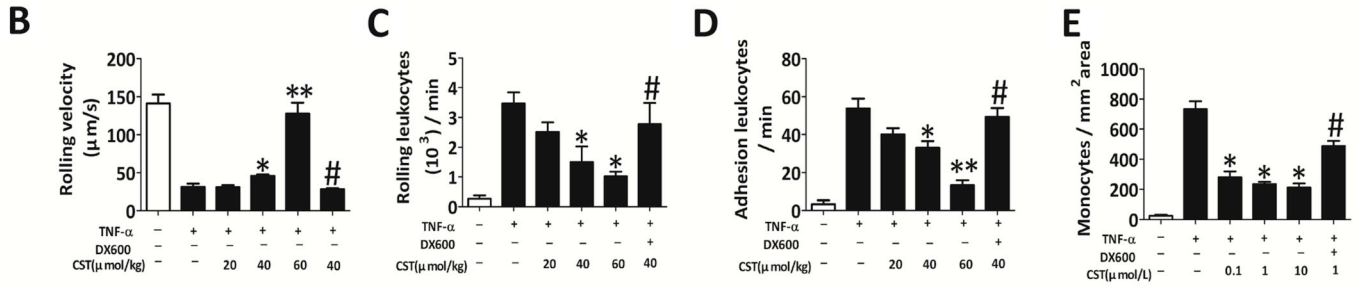

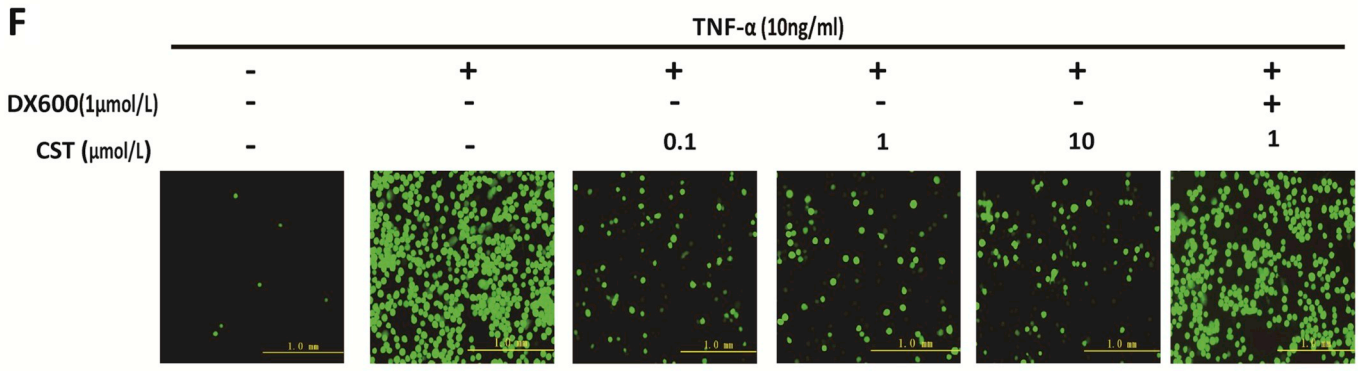

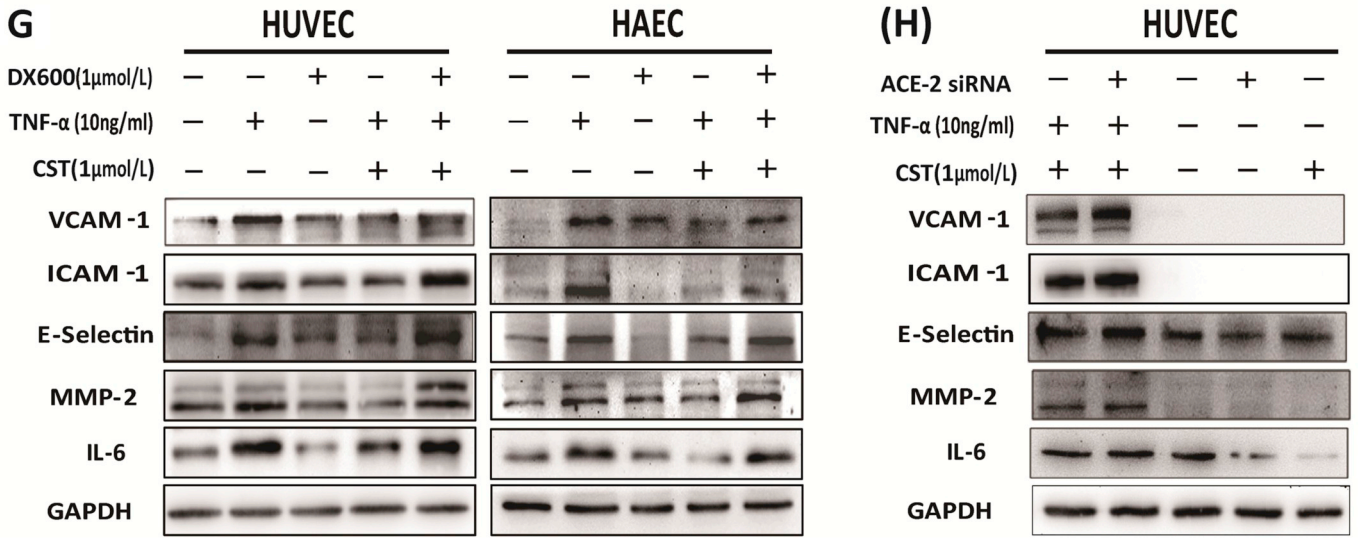

(caption on next page)

Fig. 3. ACE2 inhibition diminishes the anti-inflammatory effects of CST.
(A–D) C57BL/6 mice were subject to intraperitoneal injection of PBS or TNF-α (3 μg) in the presence or absence of DX600 (0.1 μmol/kg) and increasing doses of catestatin (CST, 20–60 μmol/kg). Representative images of the rolling leukocytes within the mesenteric venules. Scale bar = 1 mm. (B–D) Shown are quantification of the rolling velocity (B) and the number of rolling (C) and adhesion leukocytes (D). Data are expressed as the mean ± SEM ($n = 6$). *$p < 0.05$ and **$p < 0.01$ *vs.* TNF-α-treated group; #$p < 0.05$ *vs.* mice treated with TNF-α and CST (40 μmol/kg). (F) Representative images of endothelial cell-THP-1 monocyte adhesion in HUVECs treated with or without TNF-α (10 ng/mL) in the presence or absence of DX600 (1 μmol/L) and increasing doses of CST (0.1–10 μmol/L). (E) The number of adhesion monocyte per mm^2 area was quantified. Data are expressed as the mean ± SEM ($n = 6$). *$p < 0.05$ *vs.* TNF-α-treated group; #$p < 0.05$ *vs.* cells treated with TNF-α and CST (1 μmol/L). (G) Representative blots showing the expression levels of ICAM-1, VCAM-1, E-selectin, IL-6, and MMP-2 in HUVECs and HAECs treated or without TNF-α in the presence or absence of DX600 and CST. (H) HUVECs were either transfected with scramble control or ACE-2-specific siRNA for 6 h. Representative blots showing the expression levels of ICAM-1, VCAM-1, E-selectin, IL-6, and MMP-2 in the transfected HUVECs treated with or without TNF-α in the presence or absence of CST. IL-6, interleukin-6; MMP-2, matrix metalloproteinase-2; HUVECs, human umbilical vein endothelial cells; TNF-α, tumour necrosis factor-α; ICAM-1, intercellular adhesion molecule-1; VCAM-1, vascular cell adhesion molecule-1; PBS, phosphate-buffered saline; ACE2, angiotensin-converting enzyme 2; TNF-α, tumour necrosis factor-α; CST, catestatin.

3.7. CST attenuates the development of atherosclerosis

To investigate the effect of CST on atherosclerosis, $ApoE^{-/-}$ mice fed with HFD were either treated with PBS or CST in the presence or absence of DX600. After 24 weeks of HFD, the body weight, TC, and TG levels were comparable among the 3 groups (Supplementary Fig. 3A and 2C), whereas blood pressure was significantly lower in CST-treated mice than control animals ($p < 0.05$) (Supplementary Fig. 3B).

Oil red O staining showed that the total plaque area of the entire aorta was reduced in the CST-treated mice than controls, and the expression levels of the pro-inflammatory cytokines and adhesion molecules in the aorta were significantly downregulated by CST. Importantly, DX600 treatment obviously abrogated the CST-mediated protective effects (Fig. 4A, B, and F). Similarly, the cross-sectional lesion areas of atherosclerosis in the aortic roots were reduced in the CST-treated group compared with that of the controls, and this decrease was partially reversed by DX600 treatment (Fig. 4C and G). The aortic plaques in the CST-treated mice contained more collagen and fewer macrophages than those in the PBS-treated mice. DX600 co-administration partially abolished the protective effects of CST (Fig. 4D, E, H, and I).

4. Discussion

The major findings of the present study are that CST is reduced in patients with CAD and promotes endothelial dysfunction as well as the development of atherosclerosis in an ACE2-dependent mechanism. The novel points of the present study are: (1) the serum CST level is decreased in CAD patients and this decrease is related to atherosclerosis severity; (2) CST suppresses TNF-α-induced pro-inflammatory cytokine production in a dose-dependent manner and inhibits leukocyte adhesion to endothelial cells *in vitro* and *in vivo*; (3) long-term CST administration inhibits the development of atherosclerosis in $ApoE^{-/-}$ mice; and (4) the vasoprotective effects of CST involves ACE2. This study is the first to show that CST is implicated in the development of CAD and its anti-atherogenic effects are possibly mediated by ACE2.

Being identified as a peptide with catecholamine release-inhibitory activity, accumulating evidence suggests that CST a pleotropic modulator involved in multiple physiological and pathophysiological processes in the cardiovascular system. Previous studies showed that CST inhibits positive inotropic action and coronary constriction of endothelin-1 [14], as well as acts as a pro-nitric oxide agent *ex vivo* and a potent vasodilator *in vivo* [15]. Meanwhile, exogenous administration of CST was shown to limit infarct area in animal models of myocardial infarction. In line with a previous report [32], our serum analysis demonstrated that serum CST levels were negatively correlated with atherosclerosis severity, which result is consistent with a previous study reported early this year [33]. Given that chronic inflammation plays a key role in atherogenesis [34], we proposed that CST may function as an anti-inflammatory peptide independent of its anti-adrenergic properties especially in the chronic phase.

Chronic inflammation is extensively involved in the pathogenesis of atherosclerosis. TNF-α is a representative pro-inflammatory cytokine that activates nuclear factor κB and thereby promotes pro-inflammatory cytokine expressions [35]. Our study showed that TNF-α-induced inflammatory cytokines, such as IL-6, MMP-2, and adhesion molecules, including ICAM-1, VCAM-1, and E-selectin, were significantly downregulated by CST. Accordingly, endothelium-leukocyte interactions were markedly reduced in response to CST. Furthermore, CST administration led to a significantly decrease in the coverage areas of atherosclerotic lesions in aortas of $ApoE^{-/-}$ mice. A more stable plaque phenotype was also detected by CST treatment. These data support our clinical findings and suggest that CST is as novel anti-atherogenic peptide that alleviates inflammation and improves EC dysfunction.

Mechanistically, we found ACE2 expression, as well as ACE2 enzymatic activity in endothelial cells were remarkably up-regulated after CST treatment. CST is likely to shift the balance from the deleterious axis to the vasoprotective axis of RAS. The anti-inflammatory effects of CST were virtually abolished after inhibition of ACE2, either by knockdown with a specific siRNA or pharmacologically with DX600. These findings are consistent with previous reports demonstrating that ACE2 overexpression in endothelial cells decreases TNF-α-induced monocyte adhesion, whereas ACE2 silencing promotes monocyte-endothelial adhesion [36]. ACE2 is also highly expressed in coronary endothelial cells [37], and ACE2 activation promotes the formation of an anti-atherosclerotic microenvironment [38]. Consequently, endothelial inflammation and monocyte adhesion and infiltration are reduced [16,39–41]. Our results support the notion that the anti-inflammatory effects of CST are partially mediated by ACE2. Consistently, we showed that the protective effects of CST against the development of atherosclerosis in $ApoE^{-/-}$ were partially reversed by an ACE2 inhibitor.The activation of AMPK (Adenosine Monophosphate Activated Protein Kinase, AMPK) is associated with improved inflammation and may protect against vascular diseases, while this effect may lead to the activation of ACE2 [42]. A previous study has reported that CST can improve leptin signalling by phosphorylation of AMPK [43]. Due to these correlations, we come to assumption that CST may activate ACE2 by AMPK associated pathway.

4.1. Conclusions

In conclusion, we for the first time demonstrate that serum CST is lower in patients with CAD and is inversely associated with the severity of atherosclerosis. CST acts as a novel anti-atherogenic peptide by inhibiting inflammatory response and EC-leukocyte interactions in an ACE2-dependent mechanism. Further investigations are warranted to determine the underlying mechanisms modulating the crosstalk between CST and ACE2.

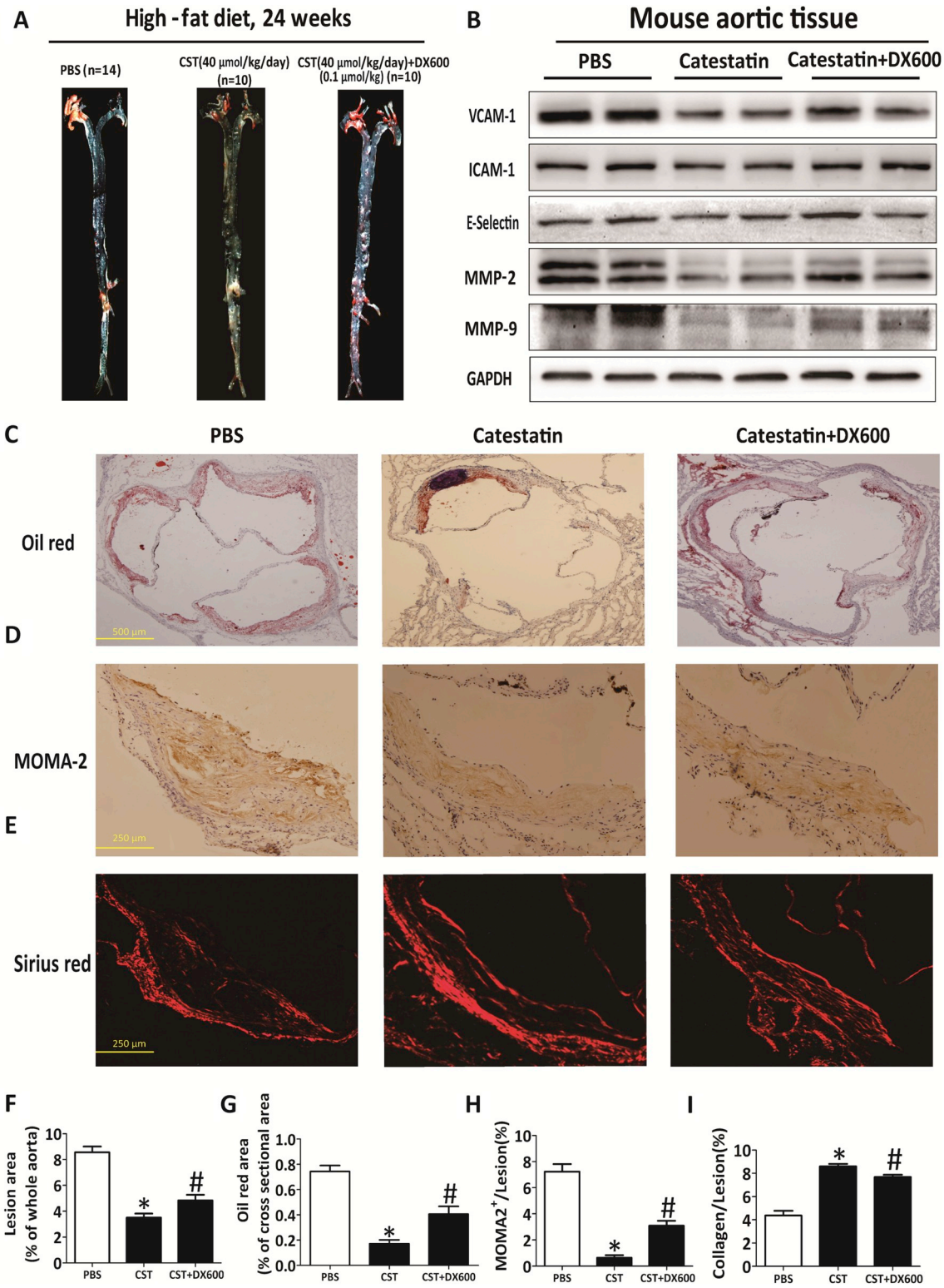

Fig. 4. Catestatin attenuates the development of atherosclerosis in an ACE2-dependent mechanism.
ApoE$^{-/-}$ mice fed with high-fat diet were either treated with PBS or catestatin (40 μmol/kg/day) in the presence or absence of DX600 (0.1 μmol/kg) for 24 weeks. (A) Representative images showing Oil Red O staining of mouse aortas of different groups. (B) Representative blots showing the expression levels of adhesion molecules (VCAM-1, ICAM-1 and E-selectin) and matrix metalloproteinases (MMP-2 and MMP9) in each group. (C–E) Representative cross-sectional images of aortic roots stained with oil red O (C), MOMA-2 (D), and Sirius red (E). Scale bar = 500 μm. (F) Quantification of atherosclerotic lesions (red areas) shown as percentage of the whole aorta. (G–I) Quantification of positively stained areas of oil red O (G), MOMA-2 (H), and Sirius red (I) in each group. Data are expressed as the means ± SEM (n = 6–8). *$p < 0.05$ *vs.* PBS-treated mice; #$p < 0.05$ *vs.* mice treated with CST alone. CST, catestatin; MOMA-2, monocyte/macrophage-2; PBS, phosphate-buffered saline.

Conflicts of interest

The authors declared they do not have anything to disclose regarding conflict of interest with respect to this manuscript.

Financial support

This study was supported by the National Natural Science Foundation of China (81370397, 81670266, and 81600198), the Research Fund for the Doctorial Innovation Program (BXJ201609), and the New Hundred Talents Program of the Shanghai Municipal Health Bureau (XBR2013100).

Author contributions

C.Y.J. and W.X.Q. wrote the main manuscript text and prepared all of the Fig.s and tables. S.X.X., Y.C.D. and Y.W.B. participated in the data analysis. J.W. wrote the manuscript and participated in the data analysis. All of the authors have read and approved the final manuscript.

Appendix A. Supplementary data

Supplementary data to this article can be found online at https://doi.org/10.1016/j.atherosclerosis.2018.12.025.

HUVECs and HAECs pretreated with catestatin (CST, 0.1–10 μmol/L) were stimulated with TNF-α (10 ng/ml) for 24 h. (A and B) Representative blots showing the expression levels of IL-6 and MMP-2. (C and D) Densitometric quantification of the Western blot results. HUVECs, open box, HAECs, closed box. (E and F) Representative blots showing the expression levels of the adhesion molecules (ICAM-1, VCAM-1, and E-selectin). (G-L) Densitometric quantification of the blots in HUVECs (G-I) and HAECs (J-L). Date are expressed as means ± SEM ($n = 6$). *$p < 0.05$, **$p < 0.01$ *vs.* cells treated with TNF-α alone. IL-6, interleukin-6; MMP-2, matrix metalloproteinase-2; HAECs, human aortic endothelial cells; HUVECs, human umbilical vein endothelial cells; TNF-α, tumour necrosis factor-α; ICAM-1, intercellular adhesion molecule-1; VCAM-1, vascular cell adhesion molecule-1.

References

[1] P. Libby, Inflammation in atherosclerosis, Nature 420 (6917) (2002) 868–874.
[2] D.I. Simon, D. Zidar, Neutrophils in atherosclerosis: alarmin evidence of a hit and run? Circ. Res. 110 (8) (2012) 1036–1038.
[3] L. Liu, W. Ding, F. Zhao, L. Shi, Y. Pang, C. Tang, Plasma levels and potential roles of catestatin in patients with coronary heart disease, Scand. Cardiovasc. J.: SCJ 47 (4) (2013) 217–224.
[4] M. Bacaner, J. Brietenbucher, J. LaBree, Prevention of ventricular fibrillation, acute myocardial infarction (myocardial necrosis), heart failure, and mortality by bretylium: is ischemic heart disease primarily adrenergic cardiovascular disease? Am. J. Therapeut. 11 (5) (2004) 366–411.
[5] S.K. Mahata, D.T. O'Connor, M. Mahata, S.H. Yoo, L. Taupenot, H. Wu, et al., Novel autocrine feedback control of catecholamine release. A discrete chromogranin a fragment is a noncompetitive nicotinic cholinergic antagonist, J. Clin. Invest. 100 (6) (1997) 1623–1633.
[6] N.R. Mahapatra, Catestatin is a novel endogenous peptide that regulates cardiac function and blood pressure, Cardiovasc. Res. 80 (3) (2008) 330–338.
[7] S.K. Mahata, M. Mahata, M.M. Fung, D.T. O'Connor, Reprint of: catestatin: a multifunctional peptide from chromogranin A, Regul. Pept. 165 (1) (2010) 52–62.
[8] Y.P. Loh, Y. Cheng, S.K. Mahata, A. Corti, B. Tota, Chromogranin A and derived peptides in health and disease, J. Mol. Neurosci.: M. Inc. 48 (2) (2012) 347–356.
[9] D.T. O'Connor, M.T. Kailasam, B.P. Kennedy, M.G. Ziegler, N. Yanaihara, R.J. Parmer, Early decline in the catecholamine release-inhibitory peptide catestatin in humans at genetic risk of hypertension, J. Hypertens. 20 (7) (2002) 1335–1345.
[10] L. Liu, W. Ding, R. Li, X. Ye, J. Zhao, J. Jiang, et al., Plasma levels and diagnostic value of catestatin in patients with heart failure, Peptides 46 (2013) 20–25.
Peng et al., 2016 F. Peng, S. Chu, W. Ding, L. Liu, J. Zhao, X. Cui, et al., The predictive value of plasma catestatin for all-cause and cardiac deaths in chronic heart failure patients, Peptides 86 (2016) 112–117.
[12] X. Wang, S. Xu, Y. Liang, D. Zhu, L. Mi, G. Wang, et al., Dramatic changes in catestatin are associated with hemodynamics in acute myocardial infarction, Biomarkers: biochemical indicators of exposure, response, and susceptibility to chemicals 16 (4) (2011) 372–377.
[13] L. Meng, J. Wang, W-h Ding, P. Han, Y. Yang, L-t Qi, et al., Plasma catestatin level in patients with acute myocardial infarction and its correlation with ventricular remodelling, Postgrad. Med. 89 (1050) (2013) 193–196.
[14] K.B. Helle, The chromogranin A-derived peptides vasostatin-I and catestatin as regulatory peptides for cardiovascular functions, Cardiovasc. Res. 85 (1) (2010) 9–16.
[15] S. Fornero, E. Bassino, M.P. Gallo, R. Ramella, R. Levi, G. Alloatti, Endothelium dependent cardiovascular effects of the Chromogranin A-derived peptides Vasostatin-1 and Catestatin, Curr. Med. Chem. 19 (24) (2012) 4059–4067.
[16] F. Jiang, J. Yang, Y. Zhang, M. Dong, S. Wang, Q. Zhang, et al., Angiotensin-converting enzyme 2 and angiotensin 1-7: novel therapeutic targets, Nat. Rev. Cardiol. 11 (7) (2014) 413–426.
[17] J. Mayito, M. Mungoma, B. Kakande, D.C. Okello, H. Wanzira, J. Kayima, et al., Angiotensin II status and sympathetic activation among hypertensive patients in Uganda: a cross-sectional study, BMC Res. Notes 8 (2015) 586.
[18] D. Weiss, J.J. Kools, W.R. Taylor, Angiotensin II-induced hypertension accelerates the development of atherosclerosis in apoE-deficient mice, Circulation 103 (3) (2001) 448–454.
[19] R.R. Gaddam, S. Chambers, M. Bhatia, ACE and ACE2 in inflammation: a tale of two enzymes, Inflamm. Allergy - Drug Targets 13 (4) (2014) 224–234.
[20] S. Salem, V. Jankowski, Y. Asare, E. Liehn, P. Welker, A. Raya-Bermudez, et al., Identification of the vasoconstriction-inhibiting factor (VIF), a potent endogenous cofactor of angiotensin II acting on the angiotensin II type 2 receptor, Circulation 131 (16) (2015) 1426–1434.
[21] Y. Goto, A. Hattori, Y. Ishii, S. Mizutani, M. Tsujimoto, Enzymatic properties of human aminopeptidase A. Regulation of its enzymatic activity by calcium and angiotensin IV, J. Biol. Chem. 281 (33) (2006) 23503–23513.
[22] T.D. Fraker Jr., S.D. Fihn, R.J. Gibbons, J. Abrams, K. Chatterjee, J. Daley, et al., Chronic angina focused update of the ACC/AHA 2002 guidelines for the management of patients with chronic stable angina: a report of the American College of Cardiology/American Heart Association Task Force on Practice Guidelines Writing Group to develop the focused update of the 2002 guidelines for the management of patients with chronic stable angina, J. Am. Coll. Cardiol. 50 (23) (2007) 2264–2274 2007.
[23] J. Taylor, ESH/ESC guidelines for the management of arterial hypertension, Eur. Heart J. 34 (28) (2013) 2108–2109 2013.
[24] M. Egger, A.G. Beer, M. Theurl, W. Schgoer, B. Hotter, T. Tatarczyk, et al., Monocyte migration: a novel effect and signaling pathways of catestatin, Eur. J. Pharmacol. 598 (1–3) (2008) 104–111.
[25] M.F. Rabbi, B. Labis, M.H. Metz-Boutigue, C.N. Bernstein, J.E. Ghia, Catestatin decreases macrophage function in two mouse models of experimental colitis, Biochem. Pharmacol. 89 (3) (2014) 386–398.
[26] S.H. Dave, J.S. Tilstra, K. Matsuoka, F. Li, T. Karrasch, J.K. Uno, et al., Amelioration of chronic murine colitis by peptide-mediated transduction of the IkappaB kinase inhibitor NEMO binding domain peptide, Journal of immunology (Baltimore, Md 179 (11) (1950) 7852–7859 2007.
[27] L. Lu, Y.N. Wang, M.C. Li, H.B. Wang, L.J. Pu, W.Q. Niu, et al., Reduced serum levels of vasostatin-2, an anti-inflammatory peptide derived from chromogranin A, are associated with the presence and severity of coronary artery disease, Eur. Heart J. 33 (18) (2012) 2297–2306.
[28] L. Lu, R.Y. Zhang, X.Q. Wang, Z.H. Liu, Y. Shen, F.H. Ding, et al., C1q/TNF-related protein-1: an adipokine marking and promoting atherosclerosis, Eur. Heart J. 37 (22) (2016) 1762–1771.
[29] W. Ying, S. Mahata, G.K. Bandyopadhyay, Z. Zhou, J. Wollam, J. Vu, et al., Catestatin inhibits obesity-induced macrophage infiltration and inflammation in the liver and suppresses hepatic glucose production, leading to improved insulin sensitivity, Diabetes 67 (5) (2018) 841–848.
[30] L. Ghazi, P. Drawz, Advances in understanding the renin-angiotensin-aldosterone system (RAAS) in blood pressure control and recent pivotal trials of RAAS blockade in heart failure and diabetic nephropathy, F1000Research 6 (2017).
[31] P. Balakumar, G. Jagadeesh, A century old renin-angiotensin system still grows with endless possibilities: AT1 receptor signaling cascades in cardiovascular physiopathology, Cell. Signal. 26 (10) (2014) 2147–2160.
[32] W. Xu, H. Yu, H. Wu, S. Li, B. Chen, W. Gao, Plasma catestatin in patients with acute coronary syndrome, Cardiology 136 (3) (2017) 164–169.
[33] M. Kojima, N. Ozawa, Y. Mori, Y. Takahashi, K. Watanabe-Kominato, R. Shirai, et al., Catestatin prevents macrophage-driven atherosclerosis but not arterial injury-induced neointimal hyperplasia, Thromb. Haemostasis 118 (1) (2018) 182–194.
[34] S. Taleb, Inflammation in atherosclerosis, Archives of cardiovascular diseases 109 (12) (2016) 708–715.
[35] T. Collins, M.A. Read, A.S. Neish, M.Z. Whitley, D. Thanos, T. Maniatis, Transcriptional regulation of endothelial cell adhesion molecules: NF-kappa B and cytokine-inducible enhancers, Faseb. J.: Off. Publ. Fed. Am. Soc. Exp. Biol. 9 (10) (1995) 899–909.
[36] L. Zhu, O.A. Carretero, J. Xu, P. Harding, N. Ramadurai, X. Gu, et al., Activation of angiotensin II type 2 receptor suppresses TNF-alpha-induced ICAM-1 via NF-small ka, CyrillicB: possible role of ACE2, Am. J. Physiol. Heart Circ. Physiol. 309 (5) (2015) H827–H834.
[37] F. Lovren, Y. Pan, A. Quan, H. Teoh, G. Wang, P.C. Shukla, et al., Angiotensin converting enzyme-2 confers endothelial protection and attenuates atherosclerosis, Am. J. Physiol. Heart Circ. Physiol. 295 (4) (2008) H1377–H1384.
[38] U. Danilczyk, U. Eriksson, G.Y. Oudit, J.M. Penninger, Physiological roles of angiotensin-converting enzyme 2, Cell. Mol. Life Sci.: CMLS 61 (21) (2004) 2714–2719.
[39] Y.H. Zhang, Q.Q. Hao, X.Y. Wang, X. Chen, N. Wang, L. Zhu, et al., ACE2 activity was increased in atherosclerotic plaque by losartan: possible relation to anti-atherosclerosis, J. Renin-Angiotensin-Aldosterone Syst. JRAAS: J. Renin-

Angiotensin-Aldosterone Syst. JRAAS 16 (2) (2015) 292–300.
[40] J.M. Yang, M. Dong, X. Meng, Y.X. Zhao, X.Y. Yang, X.L. Liu, et al., Angiotensin-(1-7) dose-dependently inhibits atherosclerotic lesion formation and enhances plaque stability by targeting vascular cells, Arterioscler. Thromb. Vasc. Biol. 33 (8) (2013) 1978–1985.
[41] C. Zhang, Y.X. Zhao, Y.H. Zhang, L. Zhu, B.P. Deng, Z.L. Zhou, et al., Angiotensin-converting enzyme 2 attenuates atherosclerotic lesions by targeting vascular cells, Proc. Natl. Acad. Sci. U. S. A 107 (36) (2010) 15886–15891.
[42] E.N. Kim, M.Y. Kim, J.H. Lim, Y. Kim, S.J. Shin, C.W. Park, et al., The protective effect of resveratrol on vascular aging by modulation of the renin-angiotensin system, Atherosclerosis 270 (2018) 123–131.
[43] G.K. Bandyopadhyay, C.U. Vu, S. Gentile, H. Lee, N. Biswas, N.W. Chi, et al., Catestatin (chromogranin A(352-372)) and novel effects on mobilization of fat from adipose tissue through regulation of adrenergic and leptin signaling, J. Biol. Chem. 287 (27) (2012) 23141–23151.